biologics

MDPI

Article

Selection and Characterization of Antibodies Recognizing Unnatural Base Pairs

Antonietta M. Lillo *, Nileena Velappan, Ruilian Wu and Madeline R. Bolding

Bioscience Division, Los Alamos National Laboratory, Los Alamos, NM 87545, USA; nileena@lanl.gov (N.V.); ruilian@lanl.gov (R.W.); mrbolding@lanl.gov (M.R.B.)
* Correspondence: alillo@lanl.gov

Abstract: Background: Introducing unnatural base pairs into a natural, double-stranded DNA construct is a powerful tool within synthetic biology. Accordingly, the ability to detect these unnatural base pairs has many applications, including the study and detection of semisynthetic organisms. **Objective and Methods**: The work described here aimed to select human antibodies for the specific recognition of Hirao's base pair dDs–dPn in various natural DNA contexts by using a combination of phage and yeast display technologies. **Results**: We selected a total of six antibodies in yeast-displayed scFv format, and further tested three of these antibodies in soluble form as minibodies and IgGs. We also describe an assay that can be used to detect plasmids containing dDs–dPn pair. **Conclusions**: Our antibodies did not afford the desired specificity or sensitivity for detection of a single unnatural base pair among thousands of natural. However, our data indicate not only that such detection is possible but also that these antibodies may be candidates for further affinity and specificity maturation.

Keywords: unnatural base pairs; Hirao's base pair; recognition of unnatural base pairs; phage display; yeast display; antibody selection

Citation: Lillo, A.M.; Velappan, N.; Wu, R.; Bolding, M.R. Selection and Characterization of Antibodies Recognizing Unnatural Base Pairs. *Biologics* **2024**, *4*, 423–443. https://doi.org/10.3390/biologics4040026

Academic Editor: Gary McLean

Received: 11 October 2024
Revised: 20 November 2024
Accepted: 25 November 2024
Published: 28 November 2024

1. Introduction

Life on Earth has been entirely built on only four nucleotides. Simply adding a few nucleotides vastly increases the possible complexity, which has implications for synthetic biology in creating aptamers and proteins with novel functions [1–4], as well as information storage within DNA [5,6]. To this end, several unnatural base pairs (UBPs) have been synthesized, mainly by teams led by Steven A. Benner, Philippe Marliere, Floyd E. Romesberg and Ichiro Hirao [7].

Incorporating UBPs into whole, semisynthetic organisms (SSOs) is a field of active study [8], and these SSOs have already proven valuable for generating therapeutics with noncanonical amino acids, which are currently undergoing clinical trials [9,10]. This work was started by Synthorx, which was subsequently acquired by Sanofi, indicating commercial interest in this burgeoning field that has much room for more complex SSOs and synthetic protein formulations [9]. The ability to quickly and specifically detect UBPs would greatly aid the development of SSOs by monitoring the conservation and amplification of UBP-containing DNA in real time. It would also allow real-time visualization of gene expression in SSOs or could simply distinguish SSOs from natural organisms.

While some efforts are underway to identify UBPs by sequencing methods [11–13], we are unaware of any previously described attempts to develop antibodies recognizing UBPs or to establish UBP immunodetection protocols.

Apart from mammalian dsDNA [14], all forms of DNA are very immunogenic in humans when presented in complexes with proteins [15]. It is therefore likely that a recombinant human antibody library could yield anti-DNA antibodies if interrogated in vitro, even with protein-free DNA. It is also possible that such antibodies could distinguish modifications such as the presence of unnatural base pairs since antibodies capable of recognizing modified nucleosides in RNA and DNA molecules have been previously obtained by animal immunization [16–19].

Phage display and yeast display are well-established technologies that allow affinity ligands (peptides, antibodies, and other proteins) to be expressed on the surface of non-lysogenic bacterial viruses (phages) or yeast, respectively [20–22]. In phage and yeast display libraries, each individual organism carries a single ligand, together with the gene encoding that ligand. This phenotype–genotype linkage enables researchers to apply a selection pressure (i.e., binding to the target of interest) and recover the genome or expand the organism that encodes the surviving ligand. Thus, this results in the progressive enrichment of the display library for clones capable of recognizing the target. Importantly, the identification of the selected ligands can be achieved by sequencing the DNA "tag" that codes for them. Phage display libraries can include as many as 10^{11} unique ligands, with each phage particle expressing between one and five copies of a single ligand. In contrast, yeast libraries tend to be smaller (typically 10^7 unique clones), while expressing roughly 30,000 copies of a single ligand per cell. The higher display level of yeasts, together with their larger physical size, results in significant advantages, among which is the ability to use flow cytometry to provide immediate feedback on the progress of a selection. A combination of phage display and yeast display affords many more affinity reagents than a single display platform [23].

These methods of interrogating large libraries through phage [24] and/or yeast [25] display technology have enabled us to select high-quality reagents against a variety of targets, including viral [26], bacterial [27,28], and mammalian proteins [29,30], as well as peptides and whole cells. Further, because some selections require exquisite specificity, we have honed our methods for pre-subtraction. This has allowed us to distinguish, for example, metastatic from non-metastatic melanoma cells [29], phosphorylated from non-phosphorylated peptides [31], and SARS-CoV-2 from SARS-CoV-1 [32]. In our most recent selections, toggling between phage and yeast display platforms has allowed us to select larger suites of affinity reagents, which, being well expressed on yeast, are also likely to be well folded and stable [33]. Finally, yeast display has facilitated the affinity maturation of our most promising anti-plague antibodies, which have shown to be protective in vivo [34].

Here, we describe the isolation of six unique human antibodies recognizing Hirao's pair, dDs–dPn (Figure 1B) [35], from a naïve antibody library derived from 40 healthy donors [36]. From this library, we used phage and yeast display technologies for their unique strengths, but also incorporated subtractive selection strategies to avoid the recognition of natural base pairs and directed selection against the dDs–dPn pair in the context of various DNA sequences. We also report on the characterization of the three best-behaved antibodies, chosen for dDs–dPn recognition specificity, the context dependency of recognition, and binding affinity. Finally, we describe immunoassay methods that could allow the detection of unnatural base pairs in plasmids, like hypothetical ones extracted from SSOs. We present evidence supporting the claim that these antibodies bind synthetic base pairs (dDs–dPn) with higher affinity than the equivalent natural base pair (dA–dT) in a manner that for two of the antibodies is independent of the surrounding sequence. Furthermore, we present evidence that FLISA might be a feasible assay for analysis of "real-world" samples.

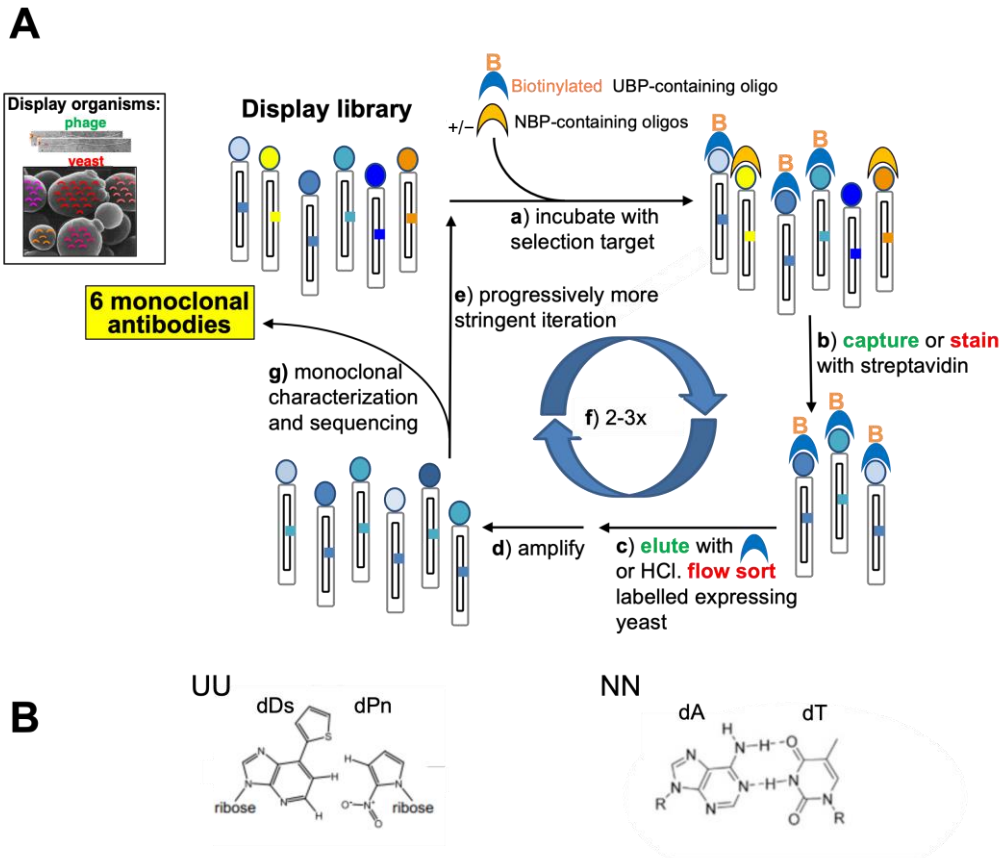

	UBP-containing sequence	NBP-containing sequence
Oligo 1	TTACTCTATCTAG**U**GATCACGGTATAC AATGAGATAGATC**U**CTAGTGCCATATG	TTACTCTATCTAG**N**GATCACGGTATAC AATGAGATAGATC**N**CTAGTGCCATATG
Oligo 2	TCTGAGTTACTTC**U**CTACAGCGACTAC AGACTCAATGAAG**U**GATGTCGCTGATG	TCTGAGTTACTTC**N**CTACAGCGACTAC AGACTCAATGAAG**N**GATGTCGCTGATG
Oligo 3	TGTGTGTTAGAAA**U**ATAGTGCCAGATC ACACACAATCTTT**U**TATCACGGTCTAG	TGTGTGTTAGAAA**N**ATAGTGCCAGATC ACACACAATCTTT**N**TATCACGGTCTAG
Oligo 4	TCTGAGTTACAAT**U**TTAGTCGCTGATG AGACTCAATGTTA**U**AATCAGCGACTAC	TCTGAGTTACAAT**N**TTAGTCGCTGATG AGACTCAATGTTA**N**AATCAGCGACTAC

Figure 1. Strategy for the selection of Hirao's base pair from display libraries. (**A**) A schematic representation of the rounds of selection for phage or yeast display is shown. Micrographs of filamentous phage (labeled in green) and yeast (labeled in red) are shown in the upper left corner, labeled. This color coding is used throughout to distinguish parts of the selection steps within the round as pertinent to either phage display (green writing) or yeast display (red writing). Display organisms (either phage or yeast) are represented schematically to highlight the displayed antibody (colored circles) and the gene coding for it (corresponding colored square inside the organism's body). Selection steps (**a**–**g**) are described in the figure. Oligos that bind to the antibodies are represented by half-moon shapes. Blue half moons represent the target, which is an oligonucleotide containing the Hirao's pair dDs-dPn (UBP, shown in panel (**B**), left). When a B is attached to a half-moon, it indicates biotin, which is used for capture or staining. Orange half-moons represent oligonucleotides containing natural base pair dA-dT (NBP, shown in panel (**B**), right). These are used for subtractive selection strategies during the incubation step of either phage or yeast display libraries. The selection of UBP-specific antibodies was encouraged by adding excess non-biotinylated UBP (blue half-moon) during the phage display elution step (**c**).

2. Materials and Methods

2.1. Hirao's Pair Synthesis

dDs Synthesis

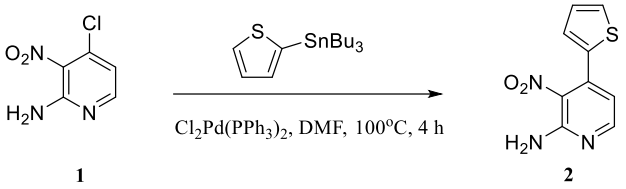

1 **2**

2-Amino-3-nitro-4-(2-thienyl) pyridine (compound **2**):

A mixture of 2-amino-3-nitro-4-chloropyridine (compound **1**) (1.74 g, 10 mmol), dichlorobis(triphenylphosphine)palladium (II) (350 mg, 0.50 mmol), and 2-(tributylstanyl) thiophene (3.82 mL, 12 mmol) in DMF (50 mL) was heated at 100 °C under argon atmosphere for 4 h. The mixture was partitioned between water and ethyl acetate. The organic layers were combined and concentrated. The residue was purified on silica gel with 40% ethyl acetate in hexanes to give 2.07 g (94%) of compound **2** as orange-colored solids. ^{1}H NMR (270 MHz, $CDCl_3$) δ 8.19 (d, 1H, *J* = 5.1 Hz), 7.47 (dd, 1H, *J* = 5.0 and 1.1 Hz), 7.14 (dd, 1H, *J* = 3.6 and 1.1 Hz), 7.10 (dd, 1H, *J* = 5.0 and 3.6 Hz), 6.78 (d, 1H, *J* = 5.1 Hz), and 5.73 (bs, 2H).

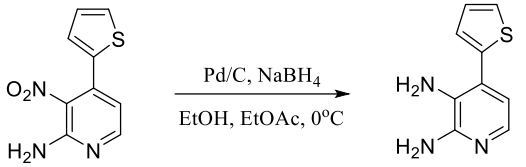

2 **3**

2,3-Diamino-4-(2-thienyl) pyridine (compound **3**):

To a mixture of compound **2** (2.06 g, 9.3 mmol) and Pd/C (466 mg, 10 wt.%) in ethanol (130 mL) and ethyl acetate (65 mL), 1 M aqueous sodium borohydride (28.0 mL) was added and stirred at 0 °C for 1 h. To the mixture, 5% aqueous ammonium chloride (43 mL) was slowly added, and the Pd/C was removed by filtration through Celite. The volatile organic solvents were removed under reduced pressure, and the residue was partitioned between ethyl acetate and water. The organic layers were combined and concentrated. The residue was purified on silica gel with 10% methanol/dichloromethane to give 1.65 g (93%) of compound **3**. ^{1}H NMR (270 MHz, $CDCl_3$) δ 7.61 (d, 1H, *J* = 5.1 Hz), 7.45 (dd, 1H, *J* = 5.1 and 1.1 Hz), 7.26 (dd, 1H, *J* = 3.5 and 1.1 Hz), 7.18 (dd, 1H, *J* = 5.1 and 3.5 Hz), 6.76 (d, 1H, *J* = 5.1 Hz), 4.68 (bs, 2H), and 3.78 (bs, 2H).

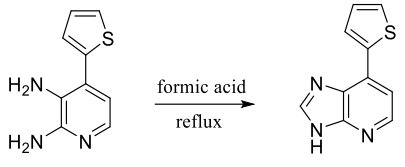

3 **4**

7-(2-Thienyl)-3H-imidazo[4,5-b] pyridine (compound **4**):

A solution of compound **3** (1.65 g, 8.63 mmol) in formic acid (26 mL) was refluxed for 12 h. Twenty-eight percent NH_4OH (40 mL) was added dropwise at 0 °C. The precipitate was filtered, washed with H_2O, and air dried to give 1.44 g (83%) of compound **4**. ^{1}H NMR (300 MHz, DMSO-d_6) δ 13.21 (s, 1H), 8.49 (s, 1H), 8.31 (m, 2H), 7.79 (dd, 1H, *J* = 1.0 and 5.1 Hz), 7.56 (d, 1H, *J* = 5.1 Hz), 7.26 (dd, 1H, *J* = 3.8 and 4.9 Hz). ^{13}C NMR (75 MHz, DMSO-d_6) 8 113.12, 128.00, 128.71, 129.24, 130.00, 131.16, 137.60, 143.44, 144.09, and 148.66.

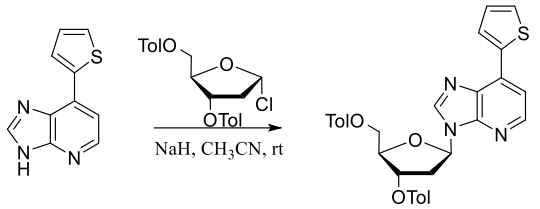

4 **5**

7-(2-Thienyl)-3-[2-deoxy-3,5-di-O-(toluoyl)-(3-D-ribofuranosyl]-3H-imidazo[4,5-b]pyridine (compound **5**):

To a solution of compound **4** (1.44 g, 7.16 mmol) in CH_3CN (115 mL), NaH (440 mg, 11.0 mmol, 60% in oil) was added at 0 °C. The resulting mixture was stirred at room temperature for 1.5 h. To this mixture, 2-deoxy-3,5-di-O-p-toluoyl-a-D-erythro-pentofuranosyl chloride (3.34 g, 8.59 mmol) was added, and the mixture was stirred for 2 h. The solvent was removed under reduced pressure, and the residue was partitioned between ethyl acetate and water. The organic layers were combined and concentrated. The residue was purified with 4% methanol in CH_2Cl_2 on silica gel to give 2.65 g (67%) of compound **5**. ^{1}H NMR (270 MHz, $CDCl_3$) δ 8.35 (d, 1H, *J* = 5.3 Hz), 8.29 (s, 1H), 8.17 (dd, 1H, *J* = 3.8 and 1.2 Hz), 7.95 (m, 4H), 7.51 (dd, 1H, *J* = 5.1 and 1.2 Hz), 7.49 (d, 1H, *J* = 5.3 Hz), 7.22 (m, 5H), 6.70 (dd, 1H, *J* = 8.6 and 5.8 Hz), 5.83 (m, 1H), 4.70 (m, 3H), 3.19 (ddd, 1H, *J* = 14.2, 8.6 and 6.4 Hz), 2.88 (ddd, 1H, *J* = 14.2, 5.8 and 2.0 Hz), 2.45 (s, 3H), and 2.39 (s, 3H).

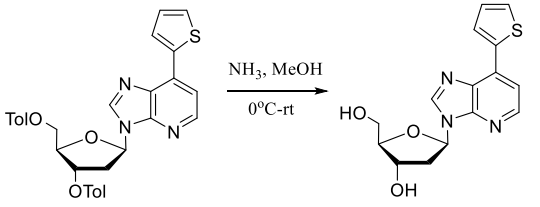

5 **6**

7-(2-Thienyl)-3-(2-deoxy-|3-D-ribofuranosyl)-3H-imidazo[4,5-b] pyridine (compound **6**):

To 2.65 g (4.79 mmol) of compound **5**, 7 M ammonia in methanol (40 mL) was added at 0 °C. The solution was stirred at room temperature for 2 days. The solvent was removed under reduced pressure, and the residue was purified with 100% ethyl acetate on silica gel to give 1.26 g (83% yield) of compound **6**. ^{1}H NMR(300MHz, DMSO-d_6) δ 8.75 (s, 1H), 8.35 (d, 1H, *J* = 5.1 Hz), 8.29 (d, 1H, *J* = 3.7 Hz), 7.83 (d, 1H, J = 5.1 Hz), 7.65 (d, 1H, *J* = 5.1 Hz), 7.27 (t, 1H, *J* = 4.2 Hz), 6.53 (t, 1H, *J* = 6.9 Hz), 5.35 (d, 1H, *J* = 4.1 Hz), 5.12 (t, 1H, *J* = 5.7 Hz), 4.45 (m, 1H), 3.91 (m, 1H), 3.60 (m, 2H), 2.79 (m, 1H), 2.34 (m, 1 H). ^{13}C NMR (75 MHz, DMSO-d_6) δ 147.10, 144.04, 143.62, 137.06, 132.00, 131.00, 129.78, 129.06, 128.07, 113.93, 87.88, 83.72, 70.80, 61.74, and 39.40.

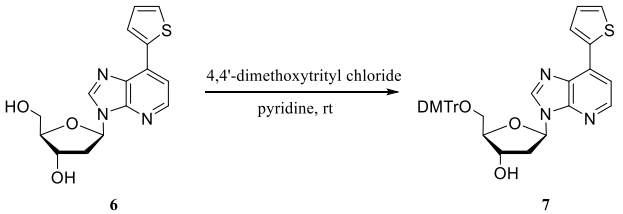

6 **7**

7-(2-Thienyl)-3-[2-deoxy-5-0-(4,4'-dimethoxytrityl)-|3-D-ribofuranosyl]-3H-imidazo[4,5-b] pyridine (compound **7**):

Compound **6** (1.26 g, 3.97 mmol) was co-evaporated three times with dry pyridine and dissolved in anhydrous pyridine (20.0 mL). To this, dimethoxytrityl chloride (1.415 g, 4.18 mmol, 1.05 eq.) was added, and the mixture was stirred overnight at room temperature; 65 mg more dimethoxytrityl chloride was added until the reaction was complete. The mixture was poured into water (50 mL) and extracted with ethyl acetate (50 mL×3). The solvent was removed under reduced pressure, and the residue was purified using 60%

ethyl acetate in hexanes to 100% ethyl acetate with 2% trimethylamine on silica gel to give 2.19 g (89%) of compound **7** as white foam. ^{1}H NMR (270 MHz, $CDCl_3$) δ 8.29 (d, 1H, *J* = 5.1 Hz), 8.24 (s, 1H), 8.19 (dd, 1H, *J* = 3.8 and 1.1 Hz), 7.51 (dd, 1H, *J* = 5.1 and 1.1 Hz), 7.46 (d, 1H, *J* = 5.1 Hz), 7.41 (m, 2H), 7.31 (m, 5H), 7.20 (m, 3H), 6.80 (m, 4H), 6.59 (dd, 1H, *J* = 6.5 and 6.2 Hz), 4.69 (m, 1H), 4.14 (m, 1H), 3.77 (s, 3H), 3.75 (s, 3H), 3.42 (dd, 1H, *J* = 10.1 and 4.6 Hz), 3.38 (dd, 1H, *J* = 10.1 and 5.4 Hz), 2.88 (m, 1H), 2.57 (ddd, 1H, *J* = 13.8, 6.5 and 4.6 Hz), and 1.97 (d, 1H, *J* = 3.5 Hz).

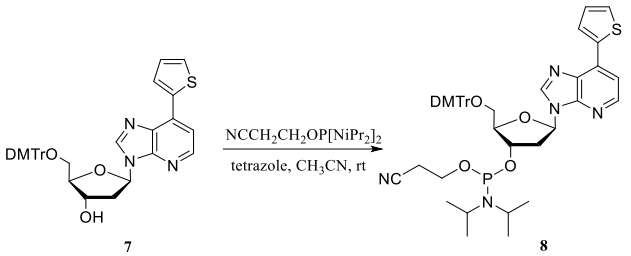

7-(2-Thienyl)-3-[2-deoxy-5-0-(4,4′-dimethoxytrityl-|3-D-ribofuranosyl]-3H-imidazo[4,5-b] pyridine 2-cyanoethyl-N,N-diisopropylphosphoramidite (compound **8**):

Compound **7** (425 mg, 0.69 mmol) was co-evaporated three times with anhydrous pyridine and then three times with anhydrous acetonitrile. This was then dissolved in anhydrous acetonitrile (4.6 mL), followed by the addition of 2-cyanoethyl tetraisopropy-lphosphorodiamidite (262 µL, 0.82 mmol) and a 0.45 M acetonitrile solution of tetrazole (1.68 mL) at room temperature. The mixture was stirred overnight at room temperature. After the addition of anhydrous methanol (90 mL), the mixture was partitioned with water and dichlromethane. The volatile organic solvents were collected and concentrated. The residue was purified using 40% ethyl acetate in hexanes with 2% triethylamine on silica to give 491 mg (87%) of compound **8** as white foam. ^{1}H NMR (270 MHz, DMSO-d_6) δ 8.67 (m, 1H), 8.29 (m, 1H), 8.25 (m, 1H), 7.83 (m, 1H), 7.64 (m, 1H), 7.30 (m, 3H), 7.17 (m, 7H), 6.77 (m, 4H), 6.54 (m, 1H), 4.82 (m, 1H), 4.14 (m, 1H), 3.81–3.47 (m, 10H), 3.21 (m, 3H), 2.82–2.64 (m, 3H) and 1.13 (m, 12H). ^{31}PNMR (109 MHz, DMSO- d_6) δ 147.55 ppm, and 146.94 ppm.

dPn Synthesis:

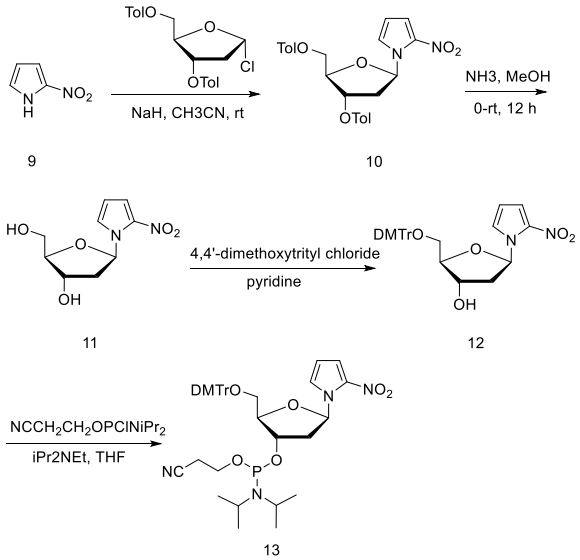

1-(2-Deoxy-a-D-ribofuranosyl)-2-nitropyrrole **10**:

To a solution of compound **9** (1.038 g 9.26 mmol) in CH_3CN (92.6 mL), NaH (370 mg, 9.26 mmol, 60% in oil) was added at 0 °C. The resulting mixture was stirred for 30 min at room temperature. To this mixture, 1-chloro-2-deoxy-3,5-di-O-toluoyl-a-D-erythro-pentofuranose (3.96 g, 10.19 mmol) was added and stirred for 2 h at room temperature.

The reaction mixture was partitioned with ethyl acetate and water. The organic layers were combined and concentrated. The residue was purified using 10–20% ethyl acetate in hexanes on silica gel to give 3.81 g (89%) of compound **10** as a white foam.

To compound **10** (3.81 g, 8.20 mmol), 7 M ammonia in methanol (60 mL) was added at 0 °C. The solution was stirred for 12 h at room temperature. The solvent was removed under reduced pressure, and the residue was purified using 4% methanol in CH_2Cl_2 on silica gel to give 1.35 g (72%) of compound **11**. ^{1}H NMR (300 MHz, DMSO-d_6) δ 7.78 (t, 1H, J = 2.4 Hz), 7.27 (dd, J = 2.1 and 4.3 Hz, 1H), 6.60 (t, J = 5.8 Hz, 1H), 6.35–6.23 (m, 1H), 5.29 (d, J = 4.3 Hz, 1H), 5.05 (t, J = 5.3 Hz, 1H), 4.24 (p, J = 4.5 Hz, 1H), 3.85 (q, J = 4.1 Hz, 1H), 3.70–3.41 (m, 2H), 2.50–2.31 (m, 3H), and 2.20 (dt, J = 13.3, 5.6 Hz, 1H).

1-[2-Deoxy-5-O-(4,4′-dimethoxytrityl)-β-D-ribofuranosyl]-2-nitropyrrole 2-Cyanoethyl-N,N-diisopropylphosphoramidite **13**.

Compound **11** (1.20 g, 5.26 mmol) was co-evaporated three times with dry pyridine and dissolved in dry pyridine (20 mL). To this solution, 4,4′-dimethoxytrityl chloride (2.66 g, 7.85 mmol) was added, and the mixture was stirred at room temperature overnight. The mixture was partitioned with ethyl acetate and water. The organic phase was washed with 5% $NaHCO_3$ and saturated NaCl, dried with Na_2SO_4, and concentrated. The product was purified with 10% ethyl acetate in CH_2Cl_2 on silica gel to give compound **12** (1.93 g, 69%). After the evaporation of compound **12** (1.93 g, 3.64 mmol) with pyridine three times, the residue was dissolved in THF (18 mL). To the mixture, N,N-diisopropylethylamine (0.95 mL, 5.48 mmol) and 2-cyano-ethyl-N,N-diisopropylamino chlorophosphoramidite (0.90 mL, 4.01 mmol) were added. The reaction mixture was stirred at room temperature for 1 h. After the addition of methanol (50 µL), the mixture was diluted with ethyl acetate/triethylamine (20:1, v/v) and then washed with 5% $NaHCO_3$ and saturated NaCl. The organic phase was dried with Na_2SO_4 and evaporated in vacuo. The product was purified by silica gel column chromatography (20–50% CH_2Cl_2 in hexane containing 2% triethylamine) to give compound **13** (1 g, 38%).

2.2. Antibody Selection

2.2.1. Antigen Design

Upon synthesizing Hirao's base pair as shown, the product was sent to Integrated DNA Technologies (Coralville, IA, USA) for incorporation into oligonucleotides. Four oligonucleotide sequences of 27 base pairs were chosen, in which the 13th nucleotide would be either an unnatural base pair (UBP) in one set or a natural base pair (NBP) in an otherwise identical set. The sequence surrounding nucleotide 14 was different for each, and they are shown in Figure 1. Each set was ordered as a biotinylated or nonbiotinylated oligo, resulting in oligos we named BU1 through BU4 (biotinylated, UBP-containing sequences 1–4), BN1 through BN4 (biotinylated, NBP-containing sequence 1–4), and nonbiotinylated counterparts.

2.2.2. Phage Display Selection

An in-house naïve human scFv library displayed on the M13 phage was used for antibody selection [36]. Four different phage display selections were carried out simultaneously using biotinylated unnatural oligos 1, 2, 3, and 4 (BU1 through BU4). The first 3 rounds of selection did not include any competitors. In round 1, the phage library (10^{13} CFU/mL in PBS, 480 µL for each quadruple selection round) was blocked by adding 5% bovine serum albumin (BSA) to a final concentration of 0.1%, and incubating for 1 h at RT. Meanwhile Streptavidin-coated magnetic beads (Dynabeads™ MyOne™ Streptavidin T1, Thermo Fisher, cat # 65601, 160 µL for each quadruple selection round) were washed according to the manufacturer's recommendations and blocked by adding 5% BSA to a final concentration of 1% and rotating for 1 h at RT. An 80 µL amount of blocked beads was collected with a magnet and separated from the blocking solution. Then, 480 µL of the blocked phage library was added to the blocked beads, and the mixture was incubated with rotation at RT for 1 h. This step allowed us to remove the phage binding to streptavidin beads. Next, 4 × 120 µL aliquots of unbound phage were incubated with 200 pmoles of

each BU at RT for 1 h in the first 4 wells of row-A of a KingFisher plate (Thermo Fisher, cat# 95040450). An 80 µL amount blocked beads was added to 720 µL PBST (PBS + 0.05 Tween-20) and aliquoted in the first 4 wells (200 µL/well) of row B of a King Fisher plate. Then, 4× 200 µL PBST (PBS + 0.05 Tween-20) aliquots were added to the first 4 wells of rows C and D; 4× 200 µL PBS (PBS + 0.05 Tween-20) aliquots were added to the first 4 wells of rows E, F, and G; and 4× 150 µL 0.1 M HCl aliquots were added to the first 4 wells of the row H. The King Fisher instrument (KF, Thermo Fisher, cat# 5400000) was programmed to perform the following steps: (1) transfer beads from row B to row A; (2) incubate beads and the library for 15 min with mild agitation; (3) transfer beads from row A to row B; (4) incubate beads for 30 s in each of the wash rows with mild agitation (3× in PBST, 3× in PBS; (5) transfer beads from row G to row H and incubate for 4 min with mild agitation (phage elution); (6) transfer bead from row H to row A; (7) stop program; (8) add 50 µL of Tris 1 M pH 8 to first 4 wells of row H (eluted phage neutralization). The phage selection round 2 conditions were the same except for longer KF washing steps (5 min instead of 30 s). Phage selection round 3 was the same as round 2 except for the lower amount of BU used during the incubation step (40 pmoles instead of 200). For round 4, we adopted two different competition strategies. In the first strategy (indicated as CI = Competition during the Incubation step) the incubation step included non-biotinylated all-natural oligos (N1–N4) in 5-fold excess (100 pmoles) with respect to BUs (20 pmoles). The KF conditions were the same as rounds 2 and 3. In the second competition strategy (indicated as CE = Competition during the Elution step), a large amount of non-biotinylated unnatural oligos (U1–U4, 1 nmoles) for phage elution instead of HCl. The rest of the conditions were the same as round 4, strategy 1 except that no N was added in the incubation step.

All rounds of selection included the amplification of the eluted phage. Ten milliliters of Omnimax T1 grown at the mid log phase (Abs_{600} or OD600 = 0.5) at 37 °C was infected with eluted phage for 1 h at 37 °C static incubation, collected by centrifugation, and plated on 2xYT agar plates containing carbenicillin (50 µg/mL) and glucose (3%). Colonies were harvested for phage amplification, using M13 helper phage and PEG precipitation according to previously described protocols [31]. Cells infected with the output phage from the 4th round of selection were used for plasmid preparation (Qiagen, #27106). ScFv-encoding genes were PCR-amplified using primers pDAN5 to pDNL6 FW (GTTCTGGTGGTGGTGGTTCTGCTAGAGGCGCGC) and pDAN5 to pDNL6 REV (GCAGTGGGTTTGGGATTGGTTTGCC). These primers added flanking sequences to the scFv gene that allow homologous recombination with the yeast display vector (pDNL6 [37]) upon yeast transformation (see section below). The PCR products were purified using the Qiagen PCR purification kit (Qiagen, #28104).

2.2.3. Yeast Display Selection

Yeast display was performed as previously described [31]. Briefly, DNA from the last output of phage selection was cloned into pDNL6 using restriction enzymes *BssH* II, *Nhe* I and *Nco* I. The resulting library was transformed into yeast, which was grown, induced, and washed. New to this work, the yeast was incubated for 1 h at room temperature with shaking in the presence of different biotinylated unnatural oligos (BU1–BU4) at concentrations from 100 nM (round 1) to as low at 10 nM (subsequent rounds). As previously described [31], the yeast with bound antigen was washed and stained with phycoerythrin-labeled anti-SV5 antibody [(Thermo Fisher Scientific Cat# MA1-34099, RRID:AB_1959285) conjugated to phycoerythrin using Lightning-Link R-PE labeling kit (Novus Bio)] and Streptavidin Alexa 633 (Thermo Fisher Scientific, S21375). It was washed and sorted using FACS Aria (Becton Dickinson). Sorted yeast was grown and used for subsequent rounds.

2.2.4. Yeast Plasmid Preparation and scFv Gene Sequencing

Plasmids from enriched yeast display libraries obtained from 3rd round sorts were isolated as previously described [31]. Briefly, yeast plasmid DNA was isolated and transformed into *E. coli*, and 192 individual colonies were submitted to GeneWiz for Sanger

sequencing service. From sequencing data, scFv sequence was analyzed, and unique clones were selected. Plasmid DNA from selected colonies was isolated and transformed back into yeast for specificity and affinity measurements.

2.2.5. Specificity of Binding and Kinetic Study of Yeast-Displayed scFvs

Yeast colonies transformed with unique scFvs were picked from SD/CAA agar plates and grown in SD/CAA liquid culture. Yeast induction and antigen staining were performed as previously described [31]. A 96-well filter plate (Millipore, #MSGVN22) was used for high-throughput analyses, using the same washing, incubation, and staining conditions indicated in the previous section. The analysis was performed either on FACS Aria or FACS ACURI 600 plus flow cytometers (Becton Dickinson). The specificity and relative affinity measurements were performed using biotinylated unnatural or natural oligos BU1 and BU2 and BN 1and BN2 at sub-saturating concentration (usually 40 nM). Dissociation constants for the highest affinity antibodies identified by this preliminary screening were obtained by (1) measuring antibody binding (y) at various concentrations of antigen; (2) plotting the data in KaleidaGraph (Version 4.5); and (3) fitting the data to the Michaelis–Menten equation adapted to antibody binding: y = m1*x/(m2 + x), where m1 = maximum antibody binding and; m2 = antibody affinity constant (K_d).

2.2.6. Conversion of scFvs to scFv-Fc (Minibody) and IgGs

This work was performed as previously described [31,37,38]. Briefly, clones that demonstrated the best affinity and specificity were chosen, and scFv genes were excised from PDNL6 and ligated into a yeast scFv-Fc expression vector pDNL9 sacB. Plasmids were transformed into *E. coli* and confirmed with sequencing. Once confirmed, plasmids were transformed into YVH10 yeast cells (in-house stocks, gift from Wittrup lab at MIT) and plated, and single colonies were grown in liquid culture. Culture supernatants were used in the ELISA-based binding assays described below.

The amino acid sequences that correspond to the variable heavy (VH) and variable light (VL) antibody regions were inserted into a standard IgG1 scaffold. The resulting protein sequences were submitted to ATUM Inc. (Newark, CA, USA) for codon-optimized back-translation, gene synthesis, and expression as full-length IgG1 antibodies in HEK293 cells. IgGs were received as PBS solutions from ATUM and stored in small aliquots at −80 °C before use in various assays.

2.3. Soluble Antibody Characterization Assays

2.3.1. Preparation of Plasmid Containing Unnatural or Natural Oligos (pU or pN)

DNA for BU2 and BN2 was obtained from IDT. Purified plasmid pDAN5 (100 µL, 600 ng/µL) was digested with NheI (NEB R3131S) for 3 h at 37 C. The plasmid was purified (Qiaquick Qiagen kit) and treated with Antarctic alkaline phosphatase (NEB M0289S) according to the vendor's recommendations. The plasmid was repurified and ligated (T7 DNA ligase, NEB M0318S) using a 10-fold excess of each sticky oligo (o/n incubation at 4 °C). Ligation product was gel-purified (Qiagen kit). The final product was a 150 µL solution of 36 ng/µL.

2.3.2. Common Steps in ELISA/FLISA

For all FLISA and ELISA assays 96-well NUNC Maxisorp plates (transparent, #442404 for ELISA or black, #43711 for FLISA) were coated with goat anti-human antibody (SouthernBiotech Cat# 2048-01, RRID:AB_2795685, 50 µg/mL, 70 µL/well, overnight incubation at 4 °C). The plates were washed once with PBS (200 µL/well). Soluble antibody was added at 70 µL/well in either yeast media (minibody) or PBS and incubated for 1 h at RT. After one more PBS wash, the plate was blocked with either 1% (FLISA) or 5% (ELISA) BSA in PBS (200 µL/well, 1 h incubation at RT), followed by 3 PBS washes. Biotinylated (ELISA) or unbiotinylated (FLISA) DNA (oligos, BU or N, or plasmids pU or pN) was then added at various concentrations in PBS, after incubation with GelRed (1:5000 dilution, in FLISA),

or in PBS (FLISA) or in Yeast Washing Buffer (YWB, 70 µL/well, ELISA). After incubation for 1 h at RT, plates were then washed 3 times with PBST and 3 times with PBS. In FLISA, washed plates were analyzed by a plate reading fluorimeter (Tecan, Ex280/Em590) upon the addition of 100 µL PBS. In ELISA, the protocol continued by adding a 1:1000 diluted solution of Streptavidin-HRP (Thermo Fisher, N100) in YWB (70 µL/well) and incubating for 1 h at RT. Upon 3 PBST and 3 PBS washes, 150 µL of TMB substrate was added to initiate the colorimetric enzymatic reaction, and 50 µL of 0.1 M H_2SO_4 was added when enough color was developed to stop the reaction. The plate was read at l = 450 nM using a plate reading spectrophotometer (Tecan). Data from either FLISA or ELISA were plotted against DNA concentration and fitted to the Michaelis–Menten equation as described in Section 2.2.5, "Specificity of Binding and Kinetic Study of Yeast-Displayed scFvs".

2.3.3. Electrophoretic Mobility Shift Assay

A 5 µM solution of IgG C05 in PBS was serially diluted twice (2-fold dilutions) and each dilution was added at a 1:1 volumetric ratio to a 5 nM solution of pU2 or pN2 in PBS. When negative control antibody (IgF1 8, [28]) was used, the highest DNA–antibody ratio was used. Mixtures were incubated at RT for 1 h and then loaded in Novex TBE acrylamide gels (Invitrogen™ EC62252BOX, 10 µL/well) and electrophoresis was run at 100 V and 18 mA. Gel was stained in 1:5000 diluted GelRed (Biotium, 41003) in PBS at RT for 1 h with mild rocking. Gel was analyzed by BioRad ChemiDoc, and band intensity was measured using ImageJ software Version 1.53. Band intensity was plotted against either DNA concentration (condition 1) or against IgG:DNA ratio (condition 2).

3. Results and Discussion

3.1. Antigen Choice and Preparation

As proof of principle, we chose to focus on Hirao's pair, dDs–dPn (hydrophobic isosteres of dA and dT), which was developed for high-fidelity PCR amplification and for proper pairing (minimal dDs mispairing with itself or dA) [35]. The synthesis of phosphoramidite dDs and dPn necessary for DNA synthesis is well established in-house (dDs and dPn 31% and 40% yield, respectively), and, based on previously unpublished work, we knew that we could send our synthesized nucleotides to Integrated DNA Technologies and easily order double-stranded oligos incorporating this base pair through their non-catalog ordering system. We therefore ordered four biotinylated and non-biotinylated double-stranded 27-mer oligonucleotides including dDs–sPs (or dA–dT) at position 13, as shown in Figure 1B (100 nmole scale). The natural DNA sequence surrounding the base pair of interest was different in each oligo, so as to provide a different context to dDs–dPn and to allow us to assess the context dependency of our selected antibodies.

3.2. Antibody Selections

Antibody selection was divided into two phases. In phase 1, we interrogated a human scFv (single chain fragment crystallizable) antibody library displayed on a phage (Figure 1A) for binding to the four biotinylated unnatural base-pair-containing oligos (BU1–BU4), represented by a blue half-moon with a B in Figure 1A.

Phages that bind the unnatural base pair form a complex with the biotinylated oligo. The complex is then captured on a streptavidin bead, washed multiple times, separated from the beads, amplified, and subjected to the next round of selection. Each oligo was used in a separate selection, in the hope that some of the antibodies selected would show up in all of the four selections, representing antibodies that recognize the unnatural base pair regardless of context. We performed four rounds of phage display selection, of which the first three did not include any competitor. In the fourth round, we attempted to eliminate antibodies that either bound to all-natural DNA or to components of the selection system other than the DNA containing dDs–dPs. To this end, we either added all-natural, non-biotinylated oligos (orange half-moon in Figure 1A) during the incubation step (these selections with competition during incubation will be denoted as CI hereafter), or we

eluted bead-captured phage with the excess non-biotinylated oligo containing dDs–dPn (B-free blue half-moon in Figure 1A; selection denoted as competition during elution, or CE, hereafter).

The outcome of each round of selection was measured by the ratio of output/input phage (Figure 2). A higher ratio indicates that the library is more highly enriched in binding antibodies. As expected, the enrichment increased from rounds 1 through 3, and it decreased at the the fourth round due to increased stringency of conditions. Yet, between round 1 and round 4, the average fold enrichment of binders was 10^5 for CI and 10^4 for CE. This enrichment reduction is expected from a competitive elution step and is typical of our previous work. Whereas HCl elution releases all binders from streptavadin-coated beads, an elution in which non-biotinylated antigen is used in excess releases phages that are bound specifically to the antigen, leaving non-specific binders on the beads. While a small percentage of true binders may remain, the CE step sacrifices throughput in favor of gaining specificity.

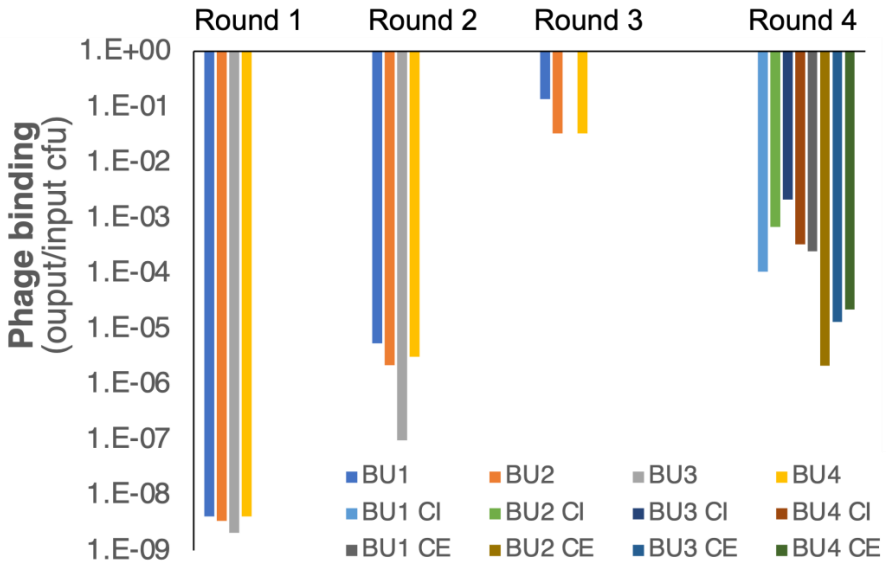

Figure 2. Results of phage display selections. Enrichment of phage-displayed libraries for target-binding antibodies (indicated as "phage binding" on the Y axis) during each round of selection is measured by the increment of the ratio of the outputted phage particle number (colony-forming units, CFUs) to inputted phage particle number (indicated as output/input CFU on the Y axis). A set of 4 different biotinylated oligos containing Hirao's unnatural base pair dDs-dPn (BU1, BU2, BU3, and BU4) were used as selection targets in the first, second, and third rounds of phage display selection (rounds 1, 2, and 3). The enrichment in target binders during each round of selection is indicated by a set of 4 colored bars (blue for BU1, orange for BU2, gray for BU3, and yellow for BU4). At round 4, the specificity of the selected antibodies was encouraged by either adding non-biotinylated natural oligos competitors during either the incubation step (CI samples) or the elution step (CE samples) instead of eluting with HCl.

Phage sublibraries obtained at the end of the fourth round of phage selection were subcloned into yeast and subjected to 2 to 3 rounds of sorting by flow cytometry. Yeast libraries from phage display selections against oligo 3 and 4 failed to grow after the first round of yeast sorting. It is possible that antibodies against these oligos were incompatible with yeast growth or that, upon interaction with these antibodies, oligos 3 and 4 penetrate yeast, resulting in growth inhibition. Neither of these theories was investigated. Only libraries selected against oligos 1 and 2 (BU1 and BU2) proceeded to yeast sorting rounds 2 and 3.

Figure 3 shows representative results obtained for one of the yeast sublibraries throughout three rounds of yeast sorting. The percentage of expressing and BU1-binding yeast increased from 5.9 at the beginning of round 1 (Figure 3C, top right graph) to 39 at the end of round 3 (Figure 3C, bottom left graph).

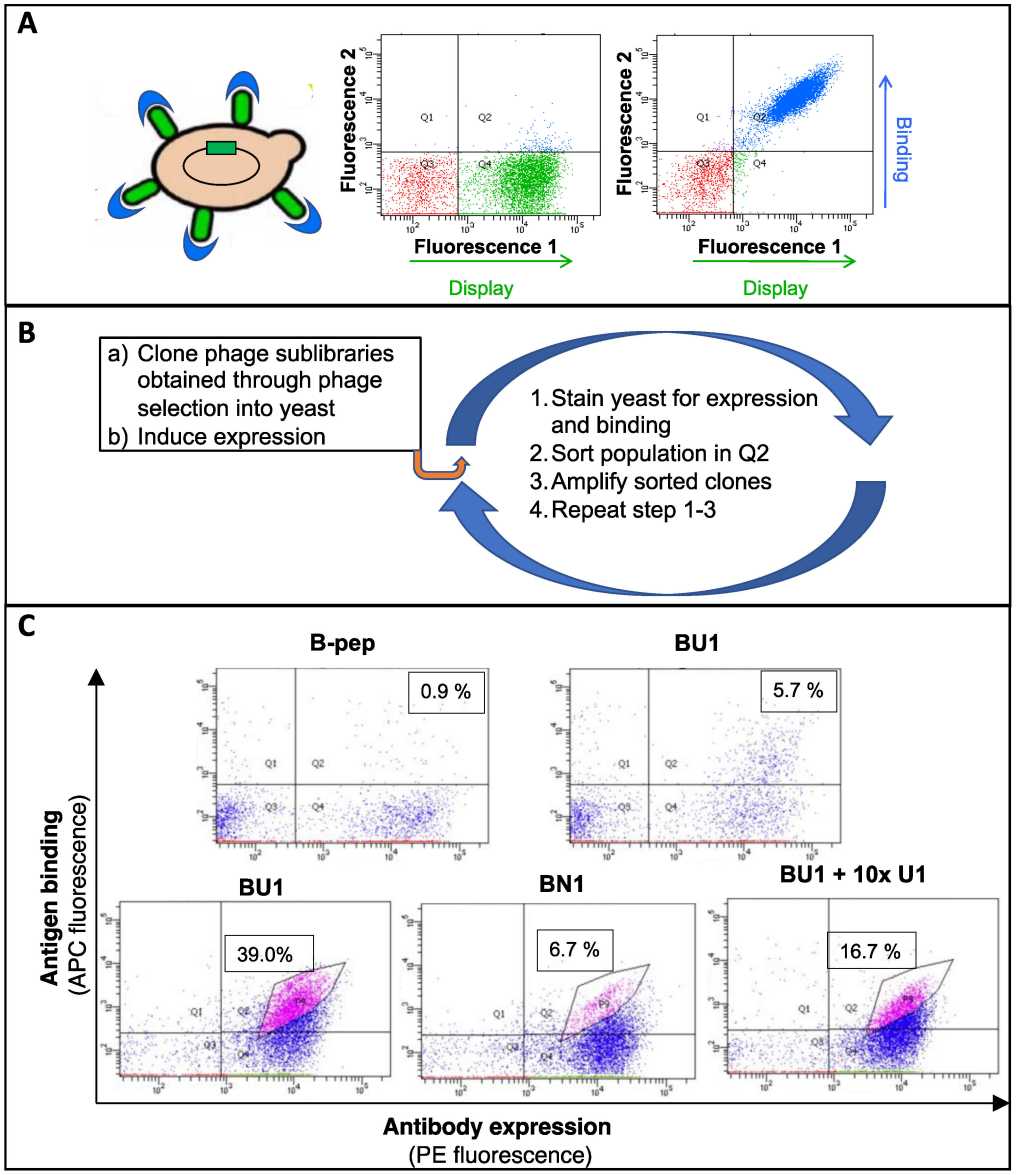

Figure 3. Selection of antibodies recognizing biotinylated unnatural oligos from yeast display libraries by flow cytometry sorting. (**A**) yeast (cartoon representation on the left) appear as dots in flow cytometry dot plots (middle and right). Yeast-displayed scFvs are expressed in tandem with a tag, which can be detected with an anti-tag antibody conjugated with fluorophore 1. This imparts "Fluorescence 1" (a proxy of expression) to the yeast, so the displaying yeast population shifts right on the *x*-axis (green dots) with respect to the non-displayed yeast population (red dots). When yeast-displayed scFvs bind to biotinylated antigens, the bound antigen can be detected with streptavidin conjugated with fluorophore 2. This imparts "fluorescence 2" (a proxy for binding) to the expressing yeast, so the displayed fraction of the displaying yeast population shifts up along the *y*-axis (blue dots). (**B**) Schematic representation of yeast selection. (**C**) Flow cytometry dot plots from the first round of selection (top graphs) show the library incubated with a negative control biotinylated peptide (B-pep) and the same library incubated with biotinylated "unnatural base pair"-containing oligo 1 (BU1). Dot plots from the third round of enrichment (bottom graphs) show the library incubated with either BU1 (left), biotinylated natural based pair-containing oligo 1 (BN1, middle), and BU1 plus a 10-fold excess of non-biotinylated "unnatural base pair"-containing oligo 1 (U1, right). Pink dot represent yeast binding to biotinylated oligos.

When the sublibrary from round 3 was stained with all BN1 instead of BU1, the percentage of expressing and binding yeast dropped to 6.7%. This demonstrated that a low

percentage of selected antibodies recognizes the all-natural sequence in BN1. Finally, the use of excess unbiotinylated dDs–dPs oligo 1 (U1) together with BU1 reduced the expressing and binding yeast population to 16.7%, demonstrating that the selected antibodies truly recognize the dDs–dPs oligo and that the interaction is not aspecific.

3.3. Single Yeast Clone Characterization

A total of 192 sorted yeast were sequenced, revealing 41 unique clones. Each of these clones was analyzed at nonsaturating concentration of BU1 or BU2 and BN1 or BN2. Based on the intensity of binding to BU and crossreaction with BN, we downselected six antibodies for futher kinetic characterization (Figure 4).

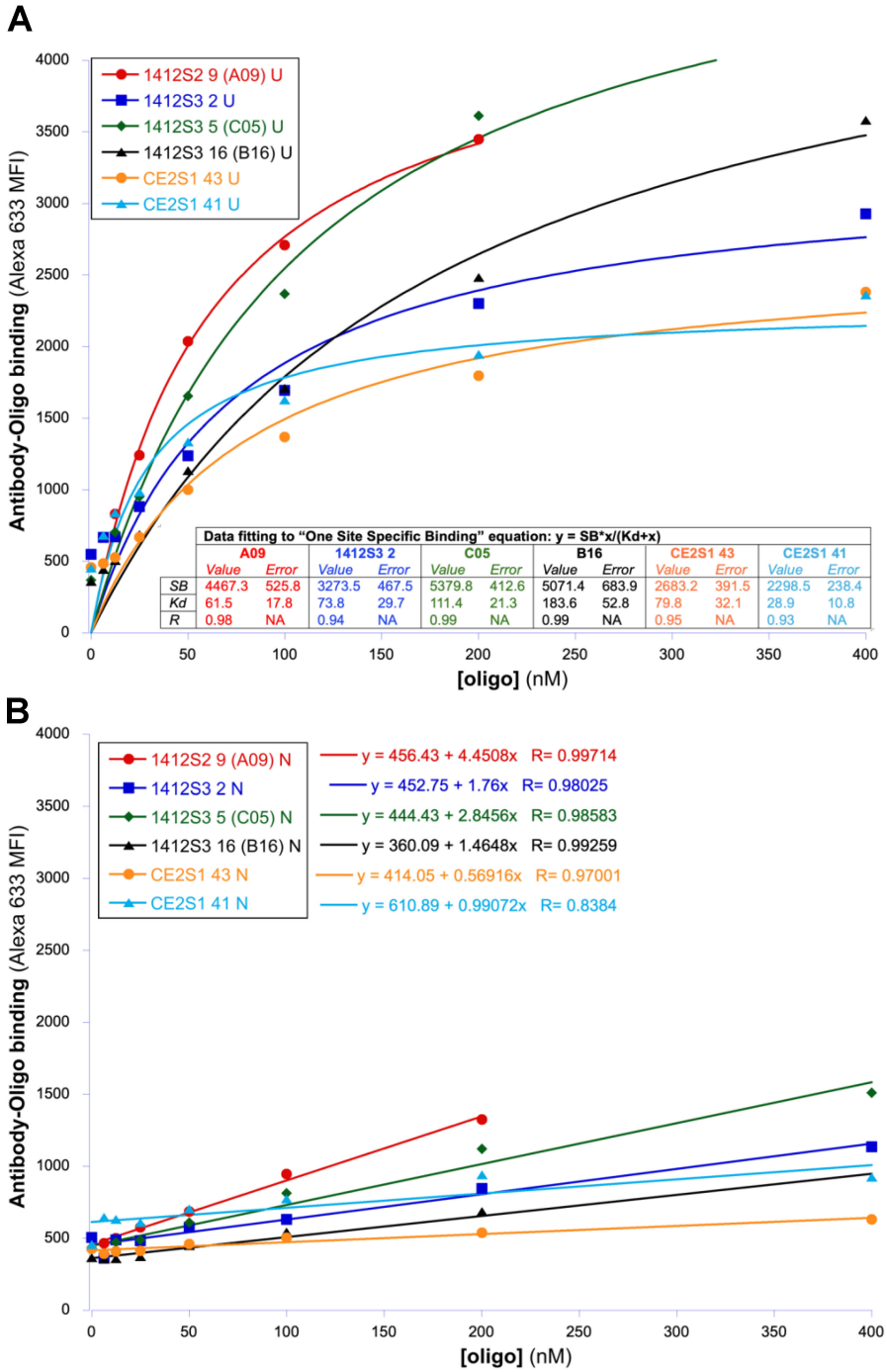

Figure 4. Kinetic characterization of yeast-displayed antibodies. Yeast-displayed scFvs were tested for binding to unnatural base-pair-containing oligo 1 (BU1, (**A**)) and natural oligo 1 (BN1, (**B**)) using

flow cytometry. Oligos were incubated with the yeast-displayed antibodies at various concentrations (X axis). Antibody–oligo binding was detected by incubation with streptavidin-Alexa 633 and by measuring the yeast-bound Alexa 633 mean fluorescence intensity (MFI, Y axis). The inset table in 4A pertains to the data points fit the one site-specific binding equation and specifies saturation binding (SB), dissociation constant (K_d, in nM), and quality of fit (R). Data points in 4B do not fit the one site-specific binding equation, but they fit a linear equation (equations for each antibody shown). The antibodies that were deemed worthy of further investigation were renamed A09, C05, and B16. These alternative names are indicated in parentheses in the legend.

Here, we show only binding to unnatural and natural oligo 1, but similar behavior was found when using oligo 2. Based on the affinity for unnatural oligos, cross-reactivity with natural oligos, and reproducibility, we chose to continue with only clones A09, C06, and B16. The sequences of these three antibodies reveal features typical of anti-DNA antibodies (Figure 5), namely arginine (R), asparagine (N), lysine (K), and tyrosine (Y) in the complementarity-determining regions (CDRs) [39]. In general, positively charged residues have been shown to interact with the negatively charged DNA backbone [40,41] via electrostatic interactions and hydrogen bonding. Further, tyrosine (Y) is found in several CDRs and is known to be enriched in paratopes recognizing charged epitopes, such as DNA [42]. Finally, we also find arginine (R) specifically in the CDRH3 region of several sequences; arginine has a strong effect on antibody interactions with nucleic acid [19].

While proper docking studies were outside of the scope of this study, we can speculate on how these residues may contribute to the binding to Hirao's base pair specifically. Structurally, Hirao's base pair contains a thiophene group that is distinct from natural base pairs. This sulfur-containing ring is expected to interact with aromatic residues in general [42]. Each of our antibodies has this potential: among other aromatic candidates, there are several YY motifs that could facilitate pi stacking, similar to thiophenes binding in other contexts, such as PDB 2HB1 [43]. A charged residue such as lysine may initiate contact, anchoring the complex to facilitate specific interactions.

A few other residues are of interest. Within sequence A09 CDRH1 is an additional aromatic motif (Y187 and Y188). As we will discuss later, A09 and C05 bind in a context-specific fashion (they do not bind to BU4 and bind with different affinity to the other BUs). Additional YY rings could facilitate binding with surrounding nucleotides in a sequence-dependent manner. The CDRH3 of C05 and CDRL3 of B16 both contain tryptophan (W), another aromatic residue, which is an uncommon amino acid and often important for binding.

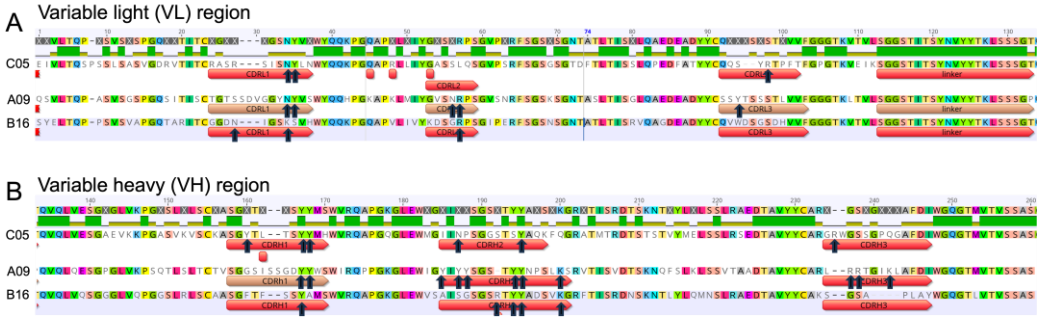

Figure 5. Alignment of the best antibody sequences. The alignment of amino acid sequences of the 3 best-performing scFvs, C05, A09, and B16 ((**A**) = variable light chain; (**B**) = variable heavy chain), are shown. The top sequences in both panels show conserved amino acids in color. The arrows point to key residues in complementarity-determining regions (CDRs) of both variable chains. The residues asparagine (N), tyrosine (Y), arginine (R), and lysine (K) are typically found in the CDRs of antibodies that recognize DNA.

3.4. Characterization of Antibodies in Soluble Form

To demonstrate that these antibodies could recognize the target antigen as soluble proteins (only yeast-displayed antibodies had been analyzed so far), we produced them as minibodies (Supplementary Figure S1A). Minibodies are scFv-Fc (single chain Fragment variable antibody–Fragment crystallizable) chimeras that are easily produced in yeast and released in the growth media. They can be used for assays without the need for purification (yeast culture supernatant is directly used in assays), and they are stable for years when stored at 4 °C.

We captured minibodies on an ELISA plate, incubated the plate with various concentrations of the four biotinylated unnatural (BU1–BU4) and natural oligos (BN1–BN4), and detected the binding with streptavidin–horse-radish peroxidase (HRP, Supplementary Figure S1B). We then plotted DNA–antibody binding versus DNA concentrations (Supplementary Figure S1C–E) and found that minibody A09 specifically bound only BU1 with linear (non-specific) background interaction with BN1 but did not bind to any other BU oligo (Supplementary Figure S1C). Minibodies B16 and C06, on the other hand, specifically bound to BU1–BU3 with linear background interaction with BN1–BN3. We can conclude that these three antibodies can distinguish BUs from BNs. Like the yeast-displayed scFv analysis (Figure 4), the A09, B16, and C06's interaction with BU is saturating, which suggests true recognition of the unnatural base pair. In contrast, interaction with BN is linear, which suggests an aspecific interaction with DNA (perhaps generic ionic interaction with DNA backbone). We can further conclude that A09's recognition of BU is context-dependent (only BU1 is recognized), whereas B16 and C09 recognize BUs in a more context-independent manner (only BU4 is not recognized).

Encouraged by these results, we decided to obtain antibodies A09, B16, and C05 in IgG format. Antibodies were produced in a good yield (58.6 through 36.8 mg for 100 mL culture; range of IgG1 yield in HEK293: 10–60 mg/100 mL), which is probably because, during yeast selection, we not only select for binding to the antigen but also for the efficiency of display, which is considered a proxy for antibody manufacturability. Figure 6 shows the kinetic analysis of IgG A09 and C05 binding to BU1–BU4 and BN1–BN4. As an IgG, antibody A09 seems to only bind specifically to BU1 and BU2. As an IgG, antibody C05 appears to bind specifically BU1, BU2, and BU3 and aspecifically to BU4. C05 also binds specifically to BN1, BN2, and BN3 (but with lower affinity and saturation binding) and aspecifically to BU4.

Kinetic parameters (K_d and saturation binding, SB, values) for antibodies in different formats are summarized in Table 1. Affinities are in the nanomolar range and show antibody C05 to be the best antibody, based on highest affinity and specificity and the lowest context-dependency. It appears that differences are more pronounced when antibodies were tested as minibodies as opposed to IgG, probably due to the lower affinities of antibodies in minibody format.

3.5. Production of Real Sample Surrogates

The immunoassays described so far used surrogate samples in the form of biotinylated short oligos. However, real samples, such as those derived from SSOs, are more likely to be non-biotinylated plasmids. Therefore, we created surrogate plasmids by cloning the synthesized natural and unnatural oligos into plasmids available in our laboratory. Rather than using restriction enzymes to cut the oligos, we synthesized them with the appropriate 5′ and 3′ overhangs that would be produced by digestion with BssHII and NheI (Supplementary Figure S2, "sticky" BU2 and BN2) and ligated into plasmids digested with these enzymes. Based on the efficiency of production, we selected plasmid pDAN5, our phage display plasmid of choice [36]. Our initial attempt to double-cut the plasmid and replace the insert with sticky BU2 or BN2 yielded very little product due to many purification steps. Therefore, we decided to cut the plasmid only with NheI and ligate only the 3′ end of the sticky oligos to the cut plasmid, yielding a linear plasmid of approximately

6 kb. The yield of this entire process was 12%. The resulting linearized plasmids were called pU and pN 1 or 2.

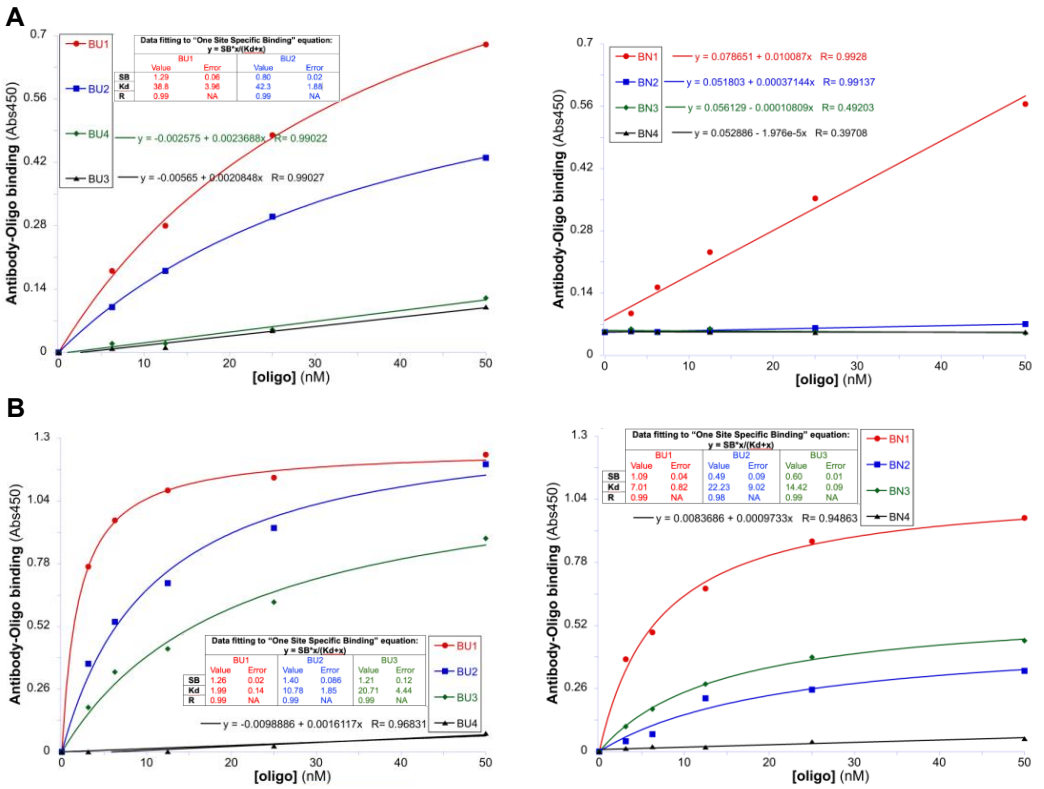

Figure 6. Kinetic analysis of antibodies in IgG format. ELISA of IgG A09 (**A**) and C05 (**B**) binding to biotinylated unnatural base pair-containing oligos (BU, left graphs) and biotinylated all-natural oligos (BN, right graphs). The antibody was immobilized on a plate and incubated with various concentrations of BU or BN (X axes). Antibody-bound BU or BN was detected with streptavidin–HRP conjugate. The absorbance at 450 nm (Abs450), the maximum absorbance of the product of horse radish peroxidase at low pH, was used as a proxy for antibody-antigen binding (Y axes). The inset tables pertain to those experiments for which data points fit the one site-specific binding equation and specify saturation binding (SB), dissociation constant (K_d, in nM), and quality of fit (R). Data points for the remaining experiments did not fit the one site-specific binding equation and either fit a linear equation (BU3 and BU4, in 6A left; BN1 and BN2, in 6A right; BU4, in 6B left; and BN4, in 6B right, equations shown) or fit neither of the two equations and are probably nonbinders (BN3 and BN4 in 6A right, notice the low R value of linear fit).

3.6. Immunoassays for Detection of Real Samples Surrogates

To detect UBPs in real sample surrogates, we wanted to explore immunoassay options with limited sample processing. Therefore, we focused on two assays not requiring biotinylation. The first assay was electrophoretic mobility shift assay (EMSA), where pU and pN were incubated with anti-UBP IgGs, stained with DNA-intercalating dyes, and analyzed for the variation of electrophoretic mobility (lower mobility = binding to antibody) by non-denaturing polyacrylamide gel electrophoresis (Supplementary Figure S3). This assay was difficult to reproduce and worked best when using pU2 and pN2 incubated with IgG C05, with plasmids at a fixed concentration and antibody at variable concentrations but always in excess with respect to plasmids (Supplementary Figure S3A). This experiment afforded fairly reproducible results as revealed by the small error bars (Supplementary Figure S3A). However, the differences between pU and pN electrophoretic shifts were significant (i.e., not within error) only at one IgG:DNA ratio (500:1).

Table 1. Kinetics of antibodies in scFv, IgG, and minibody formats.

Antibody Name	Oligo	Interaction with BUs and BNs				Antibody Format
		Affinity (Kd, nM) [a]		Saturation Binding [b]		
		BU	*BN*	*BU*	*BN*	
A09	1	61.5 ± 17.8	L/B [c]	4467.3 ± 528.8	N/A	Yeast displayed scFv
	1	38.8 ± 3.96	L/B [c]	1.3 ± 0.06	1.0 ± 0.2	IgG
	2	42.3 ± 1.88	L/B [c]	0.8 ± 0.02	N/A [e]	
	3/4	L/B	N/B [d]	N/A [f]	N/A [e]	
	1	29.6 ± 3.3	L/B [c]	0.7 ± 0.04	N/A [e]	minibody
	2/3/4	N/B	N/B [d]	N/A [f]	N/A [e]	
	1	183.6 ± 52.8	L/B [c]	5071.4 ± 683.9	N/A [e]	Yeast displayed scFv
B16	1/2/3/4	N/A [f]	N/A [f]	N/A [f]	N/A [f]	IgG
	1	48.7 ± 11.8	L/B [c]	1.1 ± 0.1	N/A [e]	minibody
	2	24.4 ± 4.0	L/B [c]	1.1 ± 0.06	N/A [e]	
	3	77.5 ± 31.5	L/B [c]	0.8 ± 0.2	N/A [e]	
	4	L/B	N/B [d]	N/A [e]	N/A [e]	
C05	1	111.4 ± 21.3	L/B [c]	5379.8 ± 412.6	N/A [e]	Yeast displayed scFv
	1	2.0 ± 0.1	7.0 ± 0.8	1.3 ± 0.02	1.1 ± 0.04	IgG
	2	10.8 ± 1.8	22.2 ± 9.0	1.4 ± 0.09	0.5 ± 0.09	
	3	20.7 ± 4.4	14.4 ± 0.9	1.2 ± 0.1	0.6 ± 0.01	
	4	L/B [c]	L/B [c]	N/A [e]	N/A [e]	
	1	39.3 ± 8.6	L/B [c]	3.1 ± 0.4	N/A [e]	minibody
	2	41.3 ± 8.6	L/B [c]	1.4 ± 0.2	N/A [e]	
	3	42.8 ± 8.6	L/B [c]	1.5 ± 0.3	N/A [e]	
	4	97.2 ± 31.3	N/B [d]	N/A [e]	N/A [e]	

[a] Kd = dissociation constant → lower Kd = higher affinity. [b] This is binding at concentrations of oligos >> than Kd and it is measured in fluorescence when analyzing yeast displayed scFv (flow cytometry) and in Abs450 when analyzing IgGs and minibodies (ELISA). [c] L/B = linear binding. This indicates aspecific interaction, i.e., not a typical anti-body-antigen interaction, Kd cannot be calculated. [d] N/B = no binding. This means that binding is at or below back-ground. [e] N/A = not available. The measurement was not performed either because binding was not detected (N/B) or because the binding was linear (L/B). [f] N/A = not available. The measurement was not performed because IgG was not available.

Considering the poor performance of EMSA, we decided to focus on a second assay, fluorescence-linked immunosorbent assay (FLISA). FLISA is very similar to the ELISA, with the major difference being the use of a fluorescent DNA dye (GelRed, that fluoresces only upon interaction with DNA), for the detection of antibody-bound DNA instead of streptavidin–HRP for the detection of antibody-bound biotinylated DNA. FLISA did not work well when using non-biotinylated oligos, probably due to the small size of the oligo and the consequent low fluorescence generated by GelRed staining. However, when using plasmids, specifically pU2 and pN2, we were able to see signals, and most importantly, we were able to see significant (i.e., not within error) differences in pU2 vs. pN2 binding, especially when antibody C05 was used (Figure 7).

Yet, the differences were smaller than what was previously detected by ELISA using oligos (BU2 and BN2) as analytes (Figure 6B). Specifically, the saturation binding value for interaction with BU2 in ELISA was three-fold higher than for the interaction with BN2. We hypothesize that the different outcomes of these two assays might be due to two factors. First, when using plasmids as opposed to oligos (i.e., a much larger natural-DNA:unnatural-DNA ratio), even low antibody cross-reaction with natural DNA obfuscates the detection of an unnatural base pair. Second, since FLISA is unfavorably affected by the blocking buffer, we did not use blocking buffer during plasmid incubation with antibody, possibly exacerbating antibody cross-reaction with natural DNA.

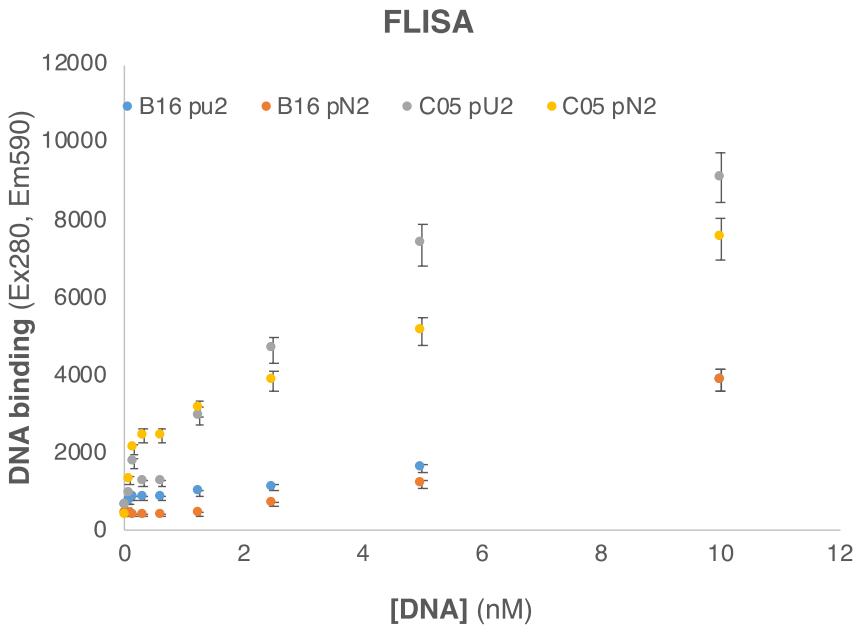

Figure 7. Detection of unnatural base-pair-containing plasmid by fluorescence-linked immunosorbent assay (FLISA). Various concentrations of GelRed pre-stained plasmids containing either unnatural plasmid 2 (pU2) or all-natural plasmid (pN2) were incubated with plate-immobilized IgG B16 or C05. Plasmid–antibody binding (indicated as DNA binding on the Y axis) was visualized by the measurement of the plate fluorescence (after extensive washing) using GelRed optimal excitation and emission wavelengths. The experiment was repeated in duplicate and the averages plus standard deviations were plotted against the plasmid concentrations.

4. Conclusions

We are the first to report on the selection of antibodies recognizing unnatural base pairs—Hirao's base pair—new exciting molecules for the expansion of the genetic code.

Using a combination of phage and yeast display, we have isolated several antibodies that appear to recognize Hirao's unnatural base pair dDs–dPn better than the dA–dT pair. It is possible that binding to dDs–dPn might include interaction with the DNA backbone, which might explain the cross-reaction of these antibodies with natural DNA. Additionally, the affinity and specificity of interaction with dDs–dPn seem to be context-specific for some of the antibodies analyzed, with antibody A09 demonstrating the best binding profile. While cross-reactivity with natural DNA does not impair specific recognition when the natural:unnatural DNA ratio is limited (e.g., when one unnatural base pair is present in a 27-mer oligonucleotide), specificity becomes obfuscated when only one unnatural base pairs is present within a ~6000 base pair plasmid.

The present goal of finding antibodies that could detect a single unnatural base pair among thousands of natural counterparts proved elusive: our antibodies did not afford the desired specificity or sensitivity for such detection. However, the short-sequence data indicate not only that such distinction is possible but also that these antibodies may be candidates for further affinity and specificity maturation, as we have previously described [28], or perhaps a rational design that incorporates classical anti-DNA residues that have been identified in disease [44] or synthetic library preparation [45]. Such improvements may enable single-UBP detection. Further, it may be of interest to determine whether multiple unnatural base pairs within a kilobase context could improve detection fidelity.

Antibodies against other forms of modified nucleotides have proven useful for understanding many aspects of cellular biology [19]. Similarly, the antibodies presented here may provide a valuable tool for the study of protein interaction with unnatural vs. natural DNA, which in turn might help in designing DNA and RNA polymerases that would lead to more stable, viable, and useful semisynthetic organisms.

Supplementary Materials: The following supporting information can be downloaded at: https://www.mdpi.com/article/10.3390/biologics4040026/s1, Figure S1: ELISA analysis of best 3 antibodies in minibody format; Figure S2: Schematic of construction of pU2 and PN2; Figure S3: Electrophoretic mobility assay (EMSA).

Author Contributions: Conceptualization, A.M.L. and N.V.; Formal analysis, A.M.L.; Investigation, A.M.L. and N.V.; Methodology, A.M.L., N.V., R.W. and M.R.B.; Supervision, A.M.L.; Writing—original draft, A.M.L.; Writing—review and editing, N.V., R.W. and M.R.B. All authors have read and agreed to the published version of the manuscript.

Funding: This work was sponsored by Other Government Agency (OGA).

Institutional Review Board Statement: This publication is approved for public release by Los Alamos National Laboratory (LA-UR-24-30249).

Informed Consent Statement: Not applicable.

Data Availability Statement: The data presented in this study are available on request from the corresponding author.

Acknowledgments: We thank Tracy Erkkila for the critical reading of the manuscript and the evaluation of experimental results.

Conflicts of Interest: The authors declare no conflicts of interest.

Abbreviations

BSA	bovine serum albumin
BU	biotinylated U
BN	biotinylated N
pU	plasmid containing U
CI	competition at the incubation step
CE	competition at the elution step
CDR	complementarity determining regions
ELISA	enzyme-linked immunosorbent assay
EMSA	electrophoretic mobility assay
FLISA	fluorescence-linked immunosorbent assay
HRP	horse radish peroxidase
IgG	Immunoglobulin G
N	all-natural DNA oligo
PAGE	polyacrylamide gel electrophoresis
PBS	phosphate-buffered saline
PCR	polymerase chain reaction
pN	plasmid containing N
scFv	single chain fragment crystallizable
SSO	semisynthetic organism
TBE	tris/borate/EDTA
UBPs	unnatural base pairs
U	unnatural base pair-containing DNA oligo

References

1. Dien, V.T.; Morris, S.E.; Karadeema, R.J.; Romesberg, F.E. Expansion of the genetic code via expansion of the genetic alphabet. *Curr. Opin. Chem. Biol.* **2018**, *46*, 196–202. [CrossRef] [PubMed]
2. Hoshika, S.; Leal, N.A.; Kim, M.-J.; Kim, M.-S.; Karalkar, N.B.; Kim, H.-J.; Bates, A.M.; Watkins, N.E., Jr.; SantaLucia, H.A.; Meyer, A.J. Hachimoji DNA and RNA: A genetic system with eight building blocks. *Science* **2019**, *363*, 884–887. [CrossRef]
3. Kimoto, M.; Yamashige, R.; Matsunaga, K.-i.; Yokoyama, S.; Hirao, I. Generation of high-affinity DNA aptamers using an expanded genetic alphabet. *Nat. Biotechnol.* **2013**, *31*, 453–457. [CrossRef]
4. Sefah, K.; Yang, Z.; Bradley, K.M.; Hoshika, S.; Jiménez, E.; Zhang, L.; Zhu, G.; Shanker, S.; Yu, F.; Turek, D. In vitro selection with artificial expanded genetic information systems. *Proc. Natl. Acad. Sci. USA* **2014**, *111*, 1449–1454. [CrossRef] [PubMed]
5. Akram, F.; Ali, H.; Laghari, A.T. Trends to store digital data in DNA: An overview. *Mol. Biol. Rep.* **2018**, *45*, 1479–1490. [CrossRef] [PubMed]

6. Ceze, L.; Nivala, J.; Strauss, K. Molecular digital data storage using DNA. *Nat. Rev. Genet.* **2019**, *20*, 456–466. [CrossRef] [PubMed]
7. de la Torre, D.; Chin, J.W. Reprogramming the genetic code. *Nat. Rev. Genet.* **2021**, *22*, 169–184. [CrossRef] [PubMed]
8. Romesberg, F.E. Creation, Optimization, and Use of Semi-Synthetic Organisms that Store and Retrieve Increased Genetic Information. *J. Mol. Biol.* **2021**, *434*, 167331. [CrossRef] [PubMed]
9. Romesberg, F.E. Discovery, implications and initial use of semi-synthetic organisms with an expanded genetic alphabet/code. *Philos. Trans. R. Soc. B* **2023**, *378*, 20220030. [CrossRef]
10. Synthorx Inc., a.S.c. *A Study Evaluating Safety and Therapeutic Activity of THOR-707 in Adult Subjects with Advanced or Metastatic Solid Tumors (THOR-707-101)*; Synthorx Inc.: La Jolla, CA, USA, 2019.
11. Craig, J.M.; Laszlo, A.H.; Derrington, I.M.; Ross, B.C.; Brinkerhoff, H.; Nova, I.C.; Doering, K.; Tickman, B.I.; Svet, M.T.; Gundlach, J.H. Direct detection of unnatural DNA nucleotides dNaM and d5SICS using the MspA nanopore. *PLoS ONE* **2015**, *10*, e0143253. [CrossRef] [PubMed]
12. Ledbetter, M.P.; Craig, J.M.; Karadeema, R.J.; Noakes, M.T.; Kim, H.C.; Abell, S.J.; Huang, J.R.; Anderson, B.A.; Krishnamurthy, R.; Gundlach, J.H. Nanopore sequencing of an expanded genetic alphabet reveals high-fidelity replication of a predominantly hydrophobic unnatural base pair. *J. Am. Chem. Soc.* **2020**, *142*, 2110–2114. [CrossRef] [PubMed]
13. Liu, Q.; Fang, L.; Yu, G.; Wang, D.; Xiao, C.-L.; Wang, K. Detection of DNA base modifications by deep recurrent neural network on Oxford Nanopore sequencing data. *Nat. Commun.* **2019**, *10*, 2449. [CrossRef]
14. Stollar, B. The origin and pathogenic role of anti-DNA autoantibodies. *Curr. Opin. Immunol.* **1990**, *2*, 607–612. [CrossRef] [PubMed]
15. Stollar, B.D. Immunochemistry of DNA. *Int. Rev. Immunol.* **1989**, *5*, 1–22. [CrossRef]
16. Reynaud, C.; Bruno, C.; Boullanger, P.; Grange, J.; Barbesti, S.; Niveleau, A. Monitoring of urinary excretion of modified nucleosides in cancer patients using a set of six monoclonal antibodies. *Cancer Lett.* **1992**, *61*, 255–262. [CrossRef] [PubMed]
17. Levine, L.; Plescia, O. Nucleic Acids as Antigens. In *Progress in Immunology*; Elsevier: Amsterdam, The Netherlands, 1971; pp. 1211–1213.
18. Erlanger, B.F.; Beiser, S.M. Antibodies specific for ribonucleosides and ribonucleotides and their reaction with DNA. *Proc. Natl. Acad. Sci. USA* **1964**, *52*, 68–74. [CrossRef]
19. Feederle, R.; Schepers, A. Antibodies specific for nucleic acid modifications. *RNA Biol.* **2017**, *14*, 1089–1098. [CrossRef]
20. Scott, J.K.; Smith, G.P. Searching for Peptide Ligands with an Epitope Library. *Science* **1990**, *249*, 386–390. [CrossRef]
21. Bradbury, A.R.M.; Marks, J.D. Antibodies from phage antibody libraries. *J. Immunol. Methods* **2004**, *290*, 29–49. [CrossRef]
22. Boder, E.T.; Wittrup, K.D. Yeast surface display for screening combinatorial polypeptide libraries. *Nat. Biotechnol.* **1997**, *15*, 553–557. [CrossRef]
23. Ferrara, F.; Soluri, M.F.; Sblattero, D. Recombinant antibody selections by combining phage and yeast display. In *Human Monoclonal Antibodies*; Springer: Berlin/Heidelberg, Germany, 2019; pp. 339–352.
24. Smith, G.P.; Petrenko, V.A. Phage display. *Chem. Rev.* **1997**, *97*, 391–410. [CrossRef] [PubMed]
25. Boder, E.T.; Wittrup, K.D. Yeast surface display for directed evolution of protein expression, affinity, and stability. *Methods Enzymol.* **2000**, *328*, 430–444.
26. Velappan, N.; Micheva-Viteva, S.; Adikari, S.H.; Waldo, G.S.; Lillo, A.M.; Bradbury, A.R. Selection and verification of antibodies against the cytoplasmic domain of M2 of influenza, a transmembrane protein. *Proc. Mabs* **2020**, *12*, 1843754. [CrossRef]
27. Lillo, A.M.; Ayriss, J.E.; Shou, Y.; Graves, S.W.; Bradbury, A.R. Development of phage-based single chain Fv antibody reagents for detection of Yersinia pestis. *PLoS ONE* **2011**, *6*, e27756. [CrossRef] [PubMed]
28. Lillo, A.M.; Velappan, N.; Kelliher, J.M.; Watts, A.J.; Merriman, S.P.; Vuyisich, G.; Lilley, L.M.; Coombs, K.E.; Mastren, T.; Teshima, M. Development of Anti-Yersinia pestis Human Antibodies with Features Required for Diagnostic and Therapeutic Applications. *ImmunoTargets Ther.* **2020**, *9*, 299. [CrossRef] [PubMed]
29. Kim, Y.; Lillo, A.M.; Steiniger, S.C.; Liu, Y.; Ballatore, C.; Anichini, A.; Mortarini, R.; Kaufmann, G.F.; Zhou, B.; Felding-Habermann, B. Targeting heat shock proteins on cancer cells: Selection, characterization, and cell-penetrating properties of a peptidic GRP78 ligand. *Biochemistry* **2006**, *45*, 9434–9444. [CrossRef]
30. Lillo, A.M.; Sun, C.; Gao, C.; Ditzel, H.; Parrish, J.; Gauss, C.-M.; Moss, J.; Felding-Habermann, B.; Wirsching, P.; Boger, D.L. A human single-chain antibody specific for integrin α3β1 capable of cell internalization and delivery of antitumor agents. *Chem. Biol.* **2004**, *11*, 897–906. [CrossRef]
31. Velappan, N.; Mahajan, A.; Naranjo, L.; Velappan, P.; Andrews, N.; Tiee, N.; Chakraborti, S.; Hemez, C.; Gaiotto, T.; Wilson, B. Selection and characterization of FcεRI phospho-ITAM specific antibodies. *Proc. MAbs* **2019**, *11*, 1206–1218. [CrossRef] [PubMed]
32. Velappan, N.L.; Nguyen, H.B.; Micheva-Viteva, S.; Bedinger, D.; Ye, C.; Mangadu, B.; Watts, A.J.; Meagher, R.; Bradfute, S.; Hu, B.; et al. Healthy humans can be a source of antibodies countering COVID-19. *Bioengineered* 2022, in press. [CrossRef]
33. Shusta, E.V.; Kieke, M.C.; Parke, E.; Kranz, D.M.; Wittrup, K.D. Yeast polypeptide fusion surface display levels predict thermal stability and soluble secretion efficiency. *J. Mol. Biol.* **1999**, *292*, 949–956. [CrossRef]
34. Li, B.; Fouts, A.E.; Stengel, K.; Luan, P.; Dillon, M.; Liang, W.-C.; Feierbach, B.; Kelley, R.F.; Hötzel, I. In vitro affinity maturation of a natural human antibody overcomes a barrier to in vivo affinity maturation. *Proc. MAbs* **2014**, *6*, 437–445. [CrossRef] [PubMed]
35. Hirao, I.; Mitsui, T.; Kimoto, M.; Yokoyama, S. An efficient unnatural base pair for PCR amplification. *J. Am. Chem. Soc.* **2007**, *129*, 15549–15555. [CrossRef] [PubMed]

36. Sblattero, D.; Bradbury, A. Exploiting recombination in single bacteria to make large phage antibody libraries. *Nat. Biotechnol.* **2000**, *18*, 75–80. [CrossRef] [PubMed]
37. Feldhaus, M.J.; Siegel, R.W.; Opresko, L.K.; Coleman, J.R.; Feldhaus, J.M.W.; Yeung, Y.A.; Cochran, J.R.; Heinzelman, P.; Colby, D.; Swers, J. Flow-cytometric isolation of human antibodies from a nonimmune Saccharomyces cerevisiae surface display library. *Nat. Biotechnol.* **2003**, *21*, 163–170. [CrossRef] [PubMed]
38. Wentz, A.E.; Shusta, E.V. A novel high-throughput screen reveals yeast genes that increase secretion of heterologous proteins. *Appl. Environ. Microbiol.* **2007**, *73*, 1189–1198. [CrossRef] [PubMed]
39. Wang, X.; Xia, Y. Anti-double Stranded DNA Antibodies: Origin, Pathogenicity, and Targeted Therapies. *Front. Immunol.* **2019**, *10*, 1667. [CrossRef]
40. Richardson, C.; Chida, A.S.; Adlowitz, D.; Silver, L.; Fox, E.; Jenks, S.A.; Palmer, E.; Wang, Y.; Heimburg-Molinaro, J.; Li, Q.-Z.; et al. Molecular Basis of 9G4 B Cell Autoreactivity in Human Systemic Lupus Erythematosus. *J. Immunol.* **2013**, *191*, 4926–4939. [CrossRef] [PubMed]
41. Schroeder, K.; Herrmann, M.; Winkler, T.H. The role of somatic hypermutation in the generation of pathogenic antibodies in SLE. *Autoimmunity* **2013**, *46*, 121–127. [CrossRef] [PubMed]
42. Akbar, R.; Robert, P.A.; Pavlovic, M.; Jeliazkov, J.R.; Snapkov, I.; Slabodkin, A.; Weber, C.R.; Scheffer, L.; Miho, E.; Haff, I.H.; et al. A compact vocabulary of paratope-epitope interactions enables predictability of antibody-antigen binding. *Cell Rep.* **2021**, *34*, 108856. [CrossRef]
43. Wan, Z.K.; Lee, J.; Xu, W.; Erbe, D.V.; Joseph-McCarthy, D.; Follows, B.C.; Zhang, Y.L. Monocyclic thiophenes as protein tyrosine phosphatase 1B inhibitors: Capturing interactions with Asp48. *Bioorganic Med. Chem. Lett.* **2006**, *16*, 4941–4945. [CrossRef]
44. Anan, Y.; Itakura, M.; Shimoda, T.; Yamaguchi, K.; Lu, P.; Nagata, K.; Dong, J.; Ueda, H.; Uchida, K. Molecular and structural basis of anti-DNA antibody specificity for pyrrolated proteins. *Commun. Biol.* **2024**, *7*, 149. [CrossRef] [PubMed]
45. Koide, S.; Sidhu, S.S. The importance of being tyrosine: Lessons in molecular recognition from minimalist synthetic binding proteins. *ACS Chem. Biol.* **2009**, *4*, 325–334. [CrossRef] [PubMed]